Tailored Wingbox Structures through Additive Manufacturing: a Summary of Ongoing Research at NASA LaRC

Bret. K. Stanford and Karen M. B. Taminger
NASA Langley Research Center, Hampton, VA
USA

bret.k.stanford@nasa.gov, karen.m.taminger@nasa.gov

ABSTRACT

The use of wingbox structural design for improved performance (i.e., fuel burn reduction) of subsonic transports is driven by two trends: reduced structural weight and increased wingspan. These two trends are in direct competition, as the increased span will exacerbate the structural reaction to aerodynamic loading, and the reduced structural weight will nominally weaken the aircraft's ability to handle this response. Novel structural configurations, enabled by recent improvements in manufacturing, may be critical toward bridging this gap. This paper summarizes pertinent activities at the NASA Langley Research Center in terms of additive manufacturing of metallic wing structures and substructures. Numerical design optimization activities are summarized as well, in order to understand where on a wingbox an additively-manufactured part may be useful and the way in which that part beneficially impacts the flight physics. The paper concludes with a discussion of how these two research paths may be better married in order to fully integrate both the benefits and realistic limitations of additive manufacturing and numerical structural design.

1.0 INTRODUCTION

A common goal across the aviation industry and aeronautics-centric government laboratories is for the next generations of subsonic transport aircraft to attain significant reductions in fuel burn, emissions, and noise pollution, relative to the current fleet of aircraft. These ambitious goals will likely only be realized with a sustained focus and investment in new numerical design tools, experimental testing procedures, and manufacturing processes, as applied to all components of the aircraft: fuselage, wing, engine, etc. The focus of the current work is on novel structural solutions for the wingbox. A fuel-optimal configuration will likely utilize a high-aspect ratio wing (for drag reduction) operating at minimum mass. As such, a key challenge is to control the passive aeroelastic behavior of this highly-flexible system by precisely tailoring the load paths through the wing. This design goal is not new, but recent advances in manufacturing of metallic structures may allow for greater and more precise control of these load paths. An important question is whether these new manufacturing tools allow for enough of a performance improvement to offset the increased manufacturing and certification costs.

The manufacturing techniques of interest here are metal additive manufacturing (AM), which encompasses a class of processes that can be used to design and construct parts using a layer-additive approach. AM processes are an outgrowth of rapid prototyping processes such as stereolithography for plastics and welding repair techniques employing laser, electron beam, or arc welding. AM offers numerous advantages, the core of which are reduced production and material costs, reduced development and lead times, and improved performance. AM processes developed over the past several years to directly produce structural metallic parts include selective laser sintering and electron beam melting [1], precision metal deposition [2], direct laser deposition processes [3], etc. The manufacturing process of interest in this work is an electron beam freeform

fabrication (EBF^3) process developed at the NASA Langley Research Center, a rapid metal deposition process that works efficiently with a variety of weldable alloys [4]-[5]. The EBF^3 process can be used to build a complex, unitized part in a layer-additive fashion (with or without compositional gradients), although the more immediate payoff is for use as a manufacturing process for adding details to components fabricated from simplified castings and forgings or plate products.

The ability to build complex unitized parts via EBF^3 may be used to enable highly-tuned and tailored wingbox structures. Furthermore, it is our view that numerical design optimization is the best way to 1) understand where on the wing such novel structures are worthwhile, 2) quantify the resulting performance improvements versus the additional manufacturing cost, and 3) understand the pertinent mechanical/dynamical/aeroelastic physics that are driving this design benefit. A numerical model of the wing is developed at a reasonable fidelity level, and a design optimization problem is set up to minimize structural mass and/or fuel burn under a set of constraints attached to various load cases. A series of optimization problems may then be solved with increasingly complex structural and material parameterizations: the simpler parameterizations represent current manufacturing practices for metallic wingbox structures, whereas the more complex parameterizations present the extremes of what a tool like EBF^3 may offer. Comparisons of the various numerical optimization results will then help answer the questions formulated above: where is EBF^3 useful, how much benefit can be derived, and what is driving this benefit? Literature, which considers numerical aircraft design (wings or panels) via optimal material and thickness grading, may be found in Refs. [6]-[10]. Topology optimization may be used to design far more complex three-dimensional parts (a solid rib web which has been replaced with a series of inter-connected lightening holes, for example); a summary of recent applications for wing structures may be found in Refs. [11] and [12].

The remainder of this work is organized as follows: a deeper discussion will be provided into the process associated with EBF^3, its limitations, and the sorts of parts it can produce. Detailed wingbox optimization studies will also be discussed to highlight and quantify the use of material grading, thickness grading, curvilinear components, and more generic topology optimization concepts. The work will conclude with a discussion related to the challenges that will need to be addressed to bridge the gap between the current state of EBF^3 and the future ability to fabricate large-scale unitized wingbox structures using processes like EBF^3 for the next generation of transports.

2.0 ELECTRON BEAM FREEFORM FABRICATION

Figure 1 shows a schematic of the primary components in an EBF^3 system. The EBF^3 process introduces metal wire feedstock into a molten pool that is created and sustained using a focused electron beam in a high vacuum environment ($1x10^{-4}$ torr or lower). The EBF^3 process is nearly 100% efficient in feedstock consumption and approaches 95% efficiency in power usage. The electron beam couples effectively with any electrically conductive material, including highly reflective alloys such as aluminum and copper. A variety of weldable alloys can be processed using EBF^3, and further development is underway to determine if non-weldable alloys can also be deposited. The EBF^3 process is capable of bulk metal deposition at deposition rates in excess of 2500 cm^3/hr (150 in^3/hr) as well as finer detailed deposition at lower deposition rates with the same piece of equipment, limited only by the positioning precision and wire feed capabilities. The diameter of the wire feedstock is the controlling factor determining the smallest detail attainable using this process: fine diameter wires may be used for adding fine details, and larger diameter wires can be used to increase deposition rate for bulk deposition. EBF^3 offers viable solutions to issues of deposition rate, process efficiency, and material compatibility for insertion into the production environment.

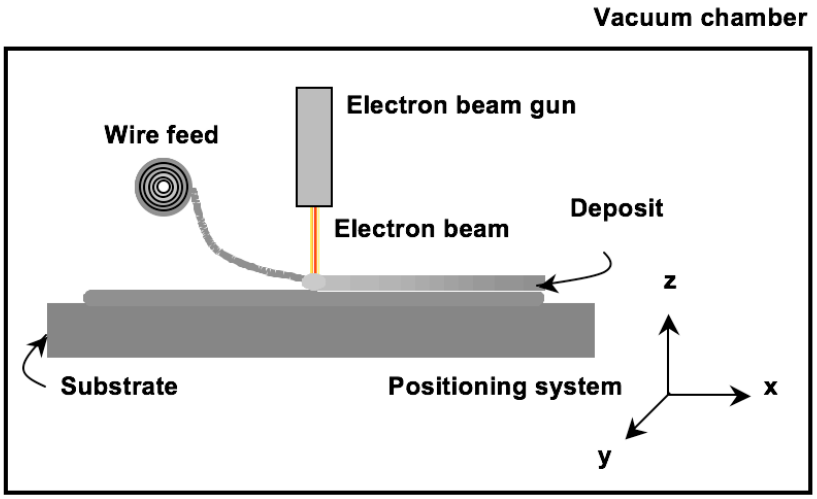

Figure 1: Schematic of electron beam freeform fabrication (EBF^3) system components.

The NASA Langley Research Center has three EBF^3 systems; the two smaller systems are housed in vacuum chambers approximately 1 m x 1 m x 1 m (35.3 cubic feet) with low power (2 kW, 20 kV accelerating voltage) electron beam guns, four-axis motion control systems, single wire feeders, and data acquisition and control systems. A larger ground-based system is a commercially-available electron beam welder that has been adapted for performing EBF^3 process development. This system includes a 42 kW, 60 kV accelerating voltage electron beam gun, a vacuum system, a positioning system, and dual wire feeders capable of independent, simultaneous operation. The two wire feeders may be loaded with either a fine and a coarse wire diameter for different feature definition, or two different alloys that may be fed simultaneously to produce components with compositional gradients.

Figure 2 shows photographs of several parts fabricated via EBF^3 using 2219 aluminum, Ti-6-4, and Inconel 718 that demonstrate the ability to program and control the process, produce parts with complex shape transitions, fabricate parts with unsupported overhangs with and without tilting the table, and the ability to control the process with varied wire feed angles into the molten pool. The parts include a variety of different nozzle shapes, airfoils, attachment nodes, and a wind tunnel model, where sizes are only limited by the size of the vacuum chamber. All of these parts have been built near-net shaped, and require a final machining to achieve the desired surface finish (although work is being pursued to eliminate finish matching). The parts fabricated using EBF^3 have demonstrated acceptable machinability and were machined using the same geometry representation used to fabricate the component to begin with [5]. An example of components with compositional gradients is shown in Figure 3, for metallic stiffeners with either grading through-depth, or grading in the plane of the stiffener.

There is a trade-off between deposition rates and feature size for materials deposited using the EBF^3 process. Additionally, higher deposition rates result in lower cooling rates that produce coarser microstructures. The tensile properties for EBF^3-deposited 2219 Al and Ti-6-4 are very consistent over a wide range of processing conditions, indicating that the tensile properties are not statistically affected by the variations within the microstructures obtained during higher versus lower heat input processing conditions. Thus, the range in microstructures documented for 2219 Al and Ti-6-4 appears to be small enough that it does not have a significant impact on the bulk tensile properties of the EBF^3-deposited materials. Note, however, that 2219 Al and Ti-6-4 have relatively simple alloy chemistries compared to many conventional alloys. It is possible that

this simplicity in composition translates to relative insensitivity to mechanical properties or microstructural variations. More work is required to characterize the range of microstructures and mechanical properties for other engineering alloys. Additional work is also required to examine other mechanical properties such as fatigue, fracture, and crack propagation to fully characterize any potential impact of the microstructural differences for all of these materials.

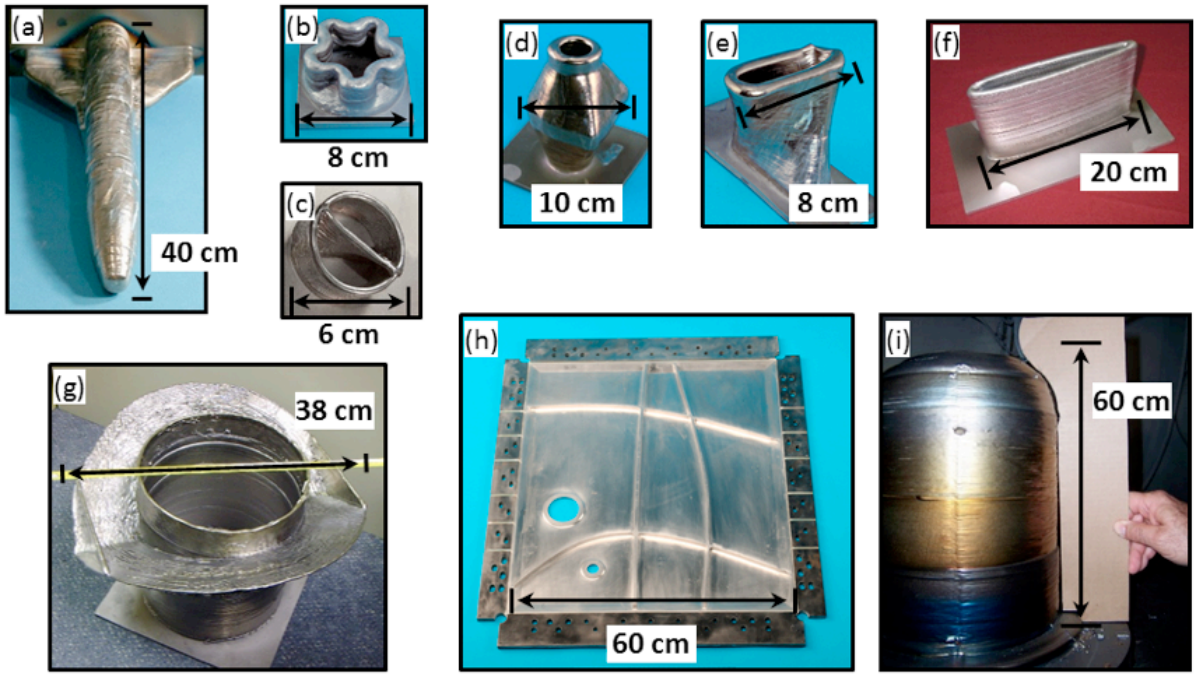

Figure 2: Examples of parts fabricated at NASA Langley using the EBF^3 process. (a) Ti-6-4 wind tunnel model; (b) 2219 Al mixer nozzle; (c) thin-walled 2219 Al mixer nozzle; (d) Ti-6-4 truss node with flat attachment surface; (e) Ti-6-4 inlet duct; (f) 2219 Al airfoil; (g) Ti-6-4 guy wire fitting; (h) 2139 Al curvilinear stiffeners deposited onto skin; (i) Inconel 718 rocket nozzle.

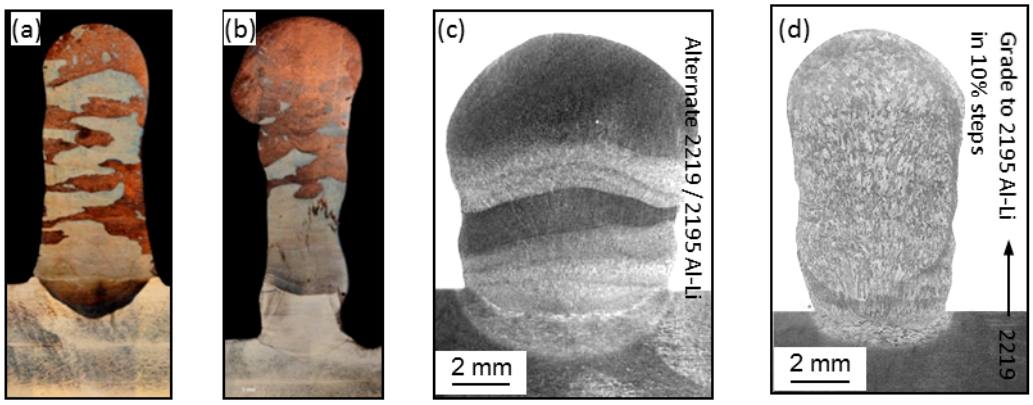

Figure 3: Example of blended compositional gradients through a metallic stiffener cross-sections: (a) Cu-Ni gradient within the stiffener plane; (b) Cu-Ni gradient through the stiffener depth; (c) 2219 Al-2195 Al-Li alternating layers; (d) 2219 Al-2195 Al-Li continuous gradient through the stiffener depth.

3.0 NUMERICAL OPTIMIZATION OF METALLIC WINGBOX STRUCTURES

A key question of interest in this work is whether the additive manufacturing EBF^3 technology demonstrated in Figure 2 and Figure 3 can be used to construct the components of a large scale wingbox for transport aircraft. The first portion of this question, considered in this section, is whether additive manufacturing is beneficial on purely physical grounds (i.e., whether a stiffener with material grading is useful for structural/aeroelastic response). If a physical basis is found lacking, then other aspects of this issue (manufacturing cost, scalability, certification: all discussed in the next section) are immaterial. All numerical examples shown in this section are demonstrated on the Common Research Model (CRM) [13], a generic transport configuration with a standard rib/spar/stiffener/skin semimonocoque wingbox.

3.1 Thickness and Material Grading Optimization

Numerical optimization involves minimizing the structural mass of the wingbox, subject to stress, buckling, and flutter constraints spread across a series of trimmed load cases. The structural parameterization (i.e., design variables) is dictated by the manufacturing process of interest. For example, the upper and lower wing skins may be divided into panel subcomponents, and the optimizer allowed to individually optimize the thickness of each panel. The panels in this case are delineated by ribs and stringers. An optimal result for such a scenario is shown in Figure 4, where peak thicknesses occur near the trailing edge wing break (where the stresses are highest) and taper to the lower bound at the tip where stresses are very low. This result does not envision additive manufacturing, but does serve as a baseline for a case that could utilize EBF^3. This latter case, shown in Figure 5, allows for detailed spatial variations in thickness within each panel. The number of design variables in Figure 5 is orders of magnitude higher than in Figure 4, but otherwise the optimization problem is the same, and so the results can be directly compared.

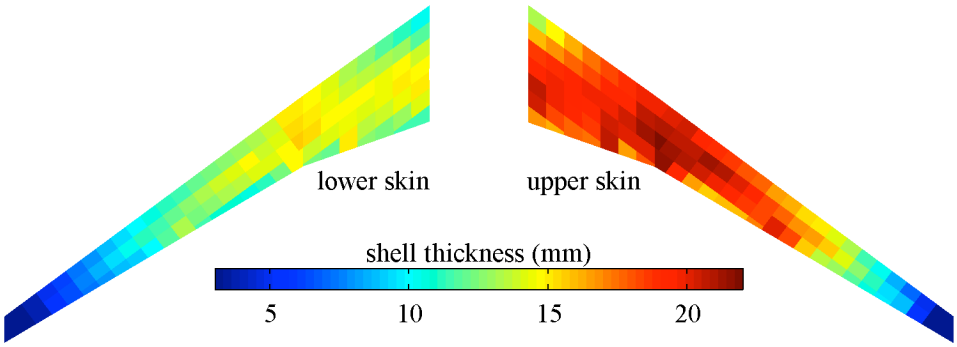

Figure 4: Optimal patchwise thickness distribution of the wing skins.

Global thickness patterns of the spatially-detailed case align with the patchwise case in Figure 4, but substantial local variations are evident, clearly driven by panel buckling. Many of the localized thickness design variables in Figure 5 are much thicker than in the baseline. These thicker members provide a *reduction* in wing mass over the baseline, however, by providing the optimizer with greater control over the local load paths and stress concentrations, and allowing for thinner members elsewhere through the skins. In summary, the optimal structural mass (objective function) of the case in Figure 5 is 8.6% lighter than the patchwise case in Figure 4, an improvement enabled by additive manufacturing.

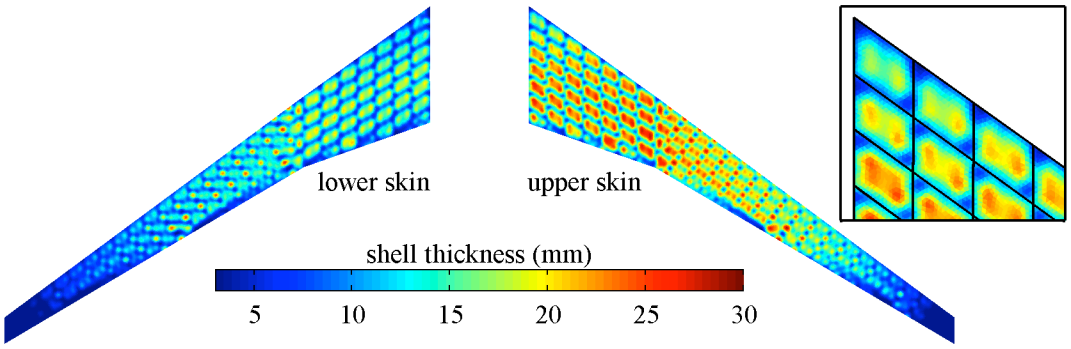

Figure 5: Optimal thickness distribution of the wing skins when detailed spatial variations are allowed.

Similar ideas may be explored for material grading. First, the result of Figure 5, an all-aluminum wing box, is used as a baseline. Then a subsequent optimization is constructed where the optimizer is allowed to control the material distribution, in addition to controlling a spatially-detailed thickness distribution. The material fraction is allowed to continuously vary between zero (100% aluminum, as in Figure 5) and one (100% titanium). Titanium is nearly twice the density of aluminum, but also has 65% higher stiffness. Although contrary to the stated optimization goal of minimized structural mass, the optimizer may still be enticed to use titanium instead of aluminum in order to exploit an increase in local stiffness, which may allow for greater reduction in mass elsewhere. The optimal result is shown in Figure 6: this design is largely composed of aluminum, but pockets of titanium are seen in the rear spar and the lower skins. The optimizer never uses 100% titanium, as this would be too heavy: peak material fractions of 32% are seen in the lower skin. Relative to the all-aluminum case in Figure 5, the graded design has a wing mass that is 3.6% lower.

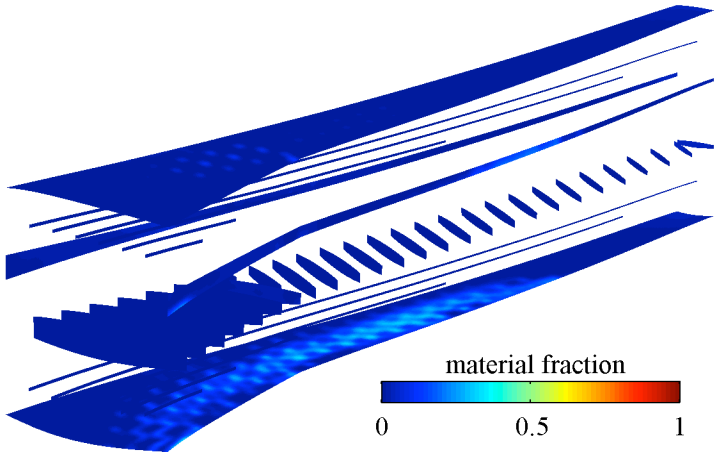

Figure 6: Optimal material fraction distribution: a value of 1 is 100% titanium; a value of 0 is 100% aluminum.

3.2 Topology Optimization

The results in section 3.1 considered only altering the thickness and material distribution throughout the wingbox components (predominately in the skins). This section considers a situation where the topology inside the wingbox itself may be optimized. Rather than a series of straight ribs and stiffeners (as used in Figure 6 for

example), these members may be bent into curvilinear paths, as demonstrated in Figure 7. EBF^3 could certainly be used to fabricate such curved members (as shown in Figure 2h) directly onto the skins and spars. Numerical optimization proceeds in a similar manner to that described above: the topology is first optimized (to minimize structural mass) using only straight ribs and stiffeners. This case is used to baseline a second case, with more design variables but the same objective and constraints, where the optimizer is allowed to utilize curved rib and stiffener paths. Preliminary results indicate a 1.2% weight reduction when curved members are utilized in place of straight members [14].

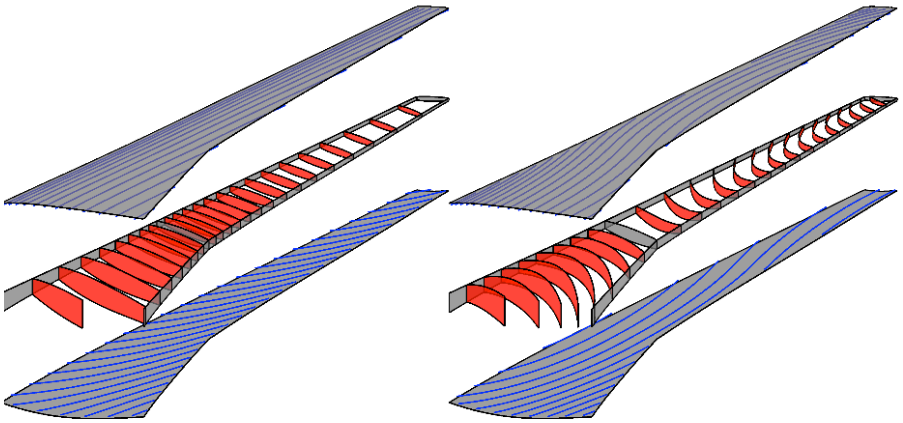

Figure 7: Sample straight (left) and curvilinear (right) stiffener/rib web components.

A second topology optimization idea would be to replace the solid web members of Figure 7 (ribs and stiffeners) with a lighter-weight concept. One could introduce lightening holes into these webs, for example, and if the amount of material removed from the webs by the optimizer is relatively large, then an additive manufacturing technique like EBF^3 would again be a reasonable choice. An example of this is shown in Figure 8, where the CRM wingbox skins are preseeded with straight, run-out blade stringers, and a topology optimizer is allowed to introduce lightening holes into the webs of these stringers in an effort to minimize structural mass (but again still meet certain stress and buckling constraints attached to a series of load cases). This exercise is conducted for both the upper and lower skin stringers (from root to tip), but only the midspan section of the upper skins is shown in Figure 8, in order to fully visualize the finely-detailed topologies.

As speculated above, the optimizer does remove the majority of the material from each web, leaving behind a series of topologies largely characterized by trapezoidal truss structures (where the long edge of the trapezoid is attached to the skins) with diagonal cross-bracing. Some of the stiffeners are removed entirely, namely those closest to the leading edge and the trailing edge of the wingbox in Figure 8. In order to baseline this topology, a second, simpler, optimization case is run, where the optimizer is forced to only allow solid full-depth stiffeners (i.e., no lightening holes). As above, this simpler baselining case is reflective of current practices for aircraft structures, and would not depend upon novel additive manufacturing processes. The optimal result in Figure 8 is 7.4% lighter than this simpler baseline case, again highlighting the efficacy of topologically-optimized wingbox structures.

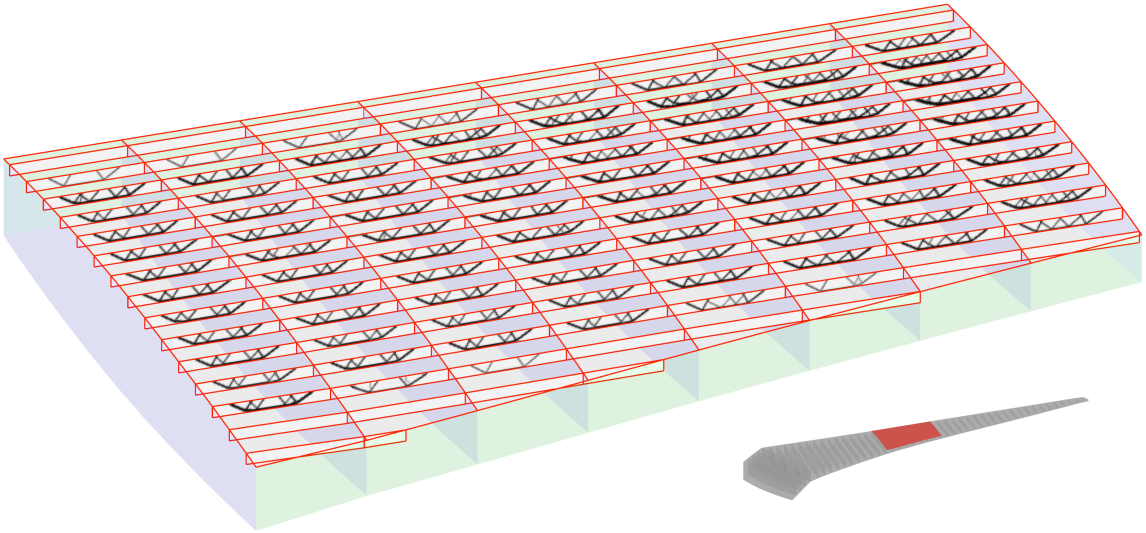

Figure 8: Topologically-optimized stiffener webs along the upper skin, near midspan.

A third type of wingbox topology optimization would involve abandoning the conventional rib-spar-stiffener concept that defines the results in Figure 7 and Figure 8, and instead allow the optimizer to generate complex three-dimensional reinforcement structures. Rather than the two-dimensional pixelated parameterization of Figure 8 (where a shell element pixel can be driven by the topology optimizer to be either solid or void), here the wingbox is populated with a large number of voxel brick elements, where each may be solid or void. The resulting optimal topology may resemble conventional components such as ribs, spars, and stiffeners, or may not, depending on the various physical metrics driving the design. This category of numerical design is substantially more complex and expensive than the previous two, owing to the large number of elements needed. The voxelated representation also makes properly baselining the optimal topologies (ideally a baseline would be a conventional rib/spar/stiffener layout) difficult. This is a significant challenge for current design, optimization, and analysis tools, but may become more realistic as tools and computational power improve. The interested reader is referred to Ref. [15] for preliminary results in this area.

4.0 MANUFACTURING LIMITATION CONSIDERATIONS DURING DESIGN

Several numerical wingbox design optimization exercises have been presented in the previous section; the successful implementation of each is hypothetically dependent upon additive manufacturing schemes such as EBF^3. Care has been taken, for each case, to baseline each optimization result against a simpler comparative result, which is reflective of standard structural practices and not dependent on novel manufacturing. The structural mass reductions demonstrated by these numerical exercises are in some cases very moderate (1.2% reduction from curvilinear ribs/stiffeners, versus straight members), and in some cases more successful (8.6% reductions from finely-detailed spatial skin thickness variations, versus patchwise thickness trends). Many of these design strategies need not be exclusive (i.e., a curved stiffener with material grading), but such synergies have not been explored here.

The structural mass reductions are important, as these could in theory be translated into manufacturing and/or operational cost (the latter through a weight versus fuel burn trade-off), and this in turn used to understand whether a given additively-manufactured part can “buy its way onto the airplane.” No effort is made here to

quantify this trade-off, though it is of course understood that large-scale fabrication of structures via large-scale additive manufacturing processes like EBF^3 is very expensive (though this cost can be expected to decrease with time) and largely unproven. This is particularly true for the complex topologically-optimized structures, such as in Figure 8. An interesting and perhaps necessary extension to the numerical optimization efforts shown here is the introduction of a cost model into the design optimization process, one which has been trained to correlate structural and/or topological feature complexity with an estimated EBF^3 manufacturing cost. Such a model, in conjunction with the implementation of a constraint that limits the total manufacturing cost, would force an optimizer to only utilize rich structural features (i.e., an aggressive spatial material grading, or a topological part with complex truss connectivity) in areas of the wingbox with the most to gain in terms of structural and aeroelastic response. In other areas of the wing where there is less to be gained from such features, the optimizer would revert to conventional structural designs, which don't rely on additive manufacturing.

A second area of improvement in the numerical work considered here would be the inclusion of manufacturing constraints during the optimization process. The inclusion of such constraints would ensure that, at least, inefficient manual design adjustment can be avoided between the numerical design phase and the experimental manufacturing phase, and at most, that the numerical optimizer does not settle on a design that cannot be built to specifications. These constraints are fairly straight-forward for the case of thickness and material grading (i.e., limiting the spatial derivative of the grading contours to that which can be reasonably achieved with EBF^3), but are more complex for topology optimization. Topology manufacturing constraints have been an active area of research (see Ref. [16], for example), in terms of overhang constraints, minimum part size and/or canal depth, part orientation, etc., but no work has been done, to the best of the authors' knowledge, for full-scale airframe structures.

5.0 CONCLUSIONS

This paper has provided a summary of current research activities at the NASA Langley Research Center in the fields of additive manufacturing (namely the electron beam freeform fabrication process) and numerical wingbox structural/aeroelastic optimization. The portions of the paper summarizing EBF^3 activities essentially demonstrates a capability that is wholly capable of producing meter-scale metallic structures, with or without material grading. The latter portions of the paper, summarizing the numerical optimization work, envisions the ways in which these EBF^3 techniques may be extended to larger-scale transport wingbox structures, in order to produce lighter-weight wings that can still withstand the required loads. Some of these manufacturing methods are found, via numerical optimization, to represent only a moderate improvement over standard manufacturing procedures (curved ribs versus standard straight ribs, for example), whereas other techniques are more successful (continuously graded skin thicknesses).

The gap between the two research fields summarized here is wide; various strategies that may help bridge this gap have been proposed, namely the inclusion of manufacturing cost and manufacturing limitation constraints during the design optimization process. Manufacturing cost constraints, which have not received much attention in the current literature, may be particularly adept at enabling situations where EBF^3 is effectively utilized for transport wingbox design. A cost constraint will force a numerical optimizer to only use EBF^3 in areas of the wingbox that can critically benefit from complex structural features (and use standard, though optimal, manufacturing practices elsewhere), and will therefore naturally limit the acreage of the resulting additively manufactured parts closer to the capabilities of current EBF^3 practices.

6.0 REFERENCES

[1] Costa, L., Vilar, R., "Laser Powder Deposition," *Rapid Prototyping* Journal, Vol. 15, No. 4, pp. 264-279, 2009.

[2] Rabinovich, J., "Net Shape Manufacturing With Metal Alloys," *Advanced Materials & Processes*, Vol. 161, No. 1, pp. 47-86, 2003.

[3] Atwood, C., Ensz, M., Greene, D., Griffith, M., Harwell, L., Reckaway, D., Romero, T., Schlienger, E., Smugeresky, J., "Laser Engineered Net Shaping (LENS^{TM}): A Tool for Direct Fabrication of Metal Parts," *Proceedings of International Congress on Applications of Lasers and Electro-Optics (ICALEO)*, Orlando, Florida, November 16-19, 1998.

[4] Taminger, K., Hafley, R., "Characterization of 2219 Aluminium Produced by Electron Beam Freeform Fabrication," *Proceedings of 13th Solid Freeform Fabrication Symposium*, Austin, Texas, August 5-7, 2002.

[5] Taminger, K., Hafley, R., "Electron Beam Freeform Fabrication for Cost Effective Near-Net Shape Manufacturing," *NATO/RTO AVT-139 Specialists' Meeting on Cost Effective Manufacture via Net Shape Processing*, Amsterdam, Netherlands, May 15-17, 2006.

[6] Stere, A., Librescu, L., "Nonlinear Thermoaeroelastic Modeling of Advanced Aircraft Wings made of Functionally Graded Materials," *AIAA Structures, Structural Dynamics, and Materials Conference*, Atlanta, Georgia, April 3-6, 2000.

[7] Librescu, L., Maalawi, K., "Material Grading for Improved Aeroelastic Stability in Composite Wings," *Journal of Mechanics of Materials and Structures*, Vol. 2, No. 7, pp. 1381-1394, 2007.

[8] Marzocca, P., Fazelzadeh, S., Hosseini, M., "A Review of Nonlinear Aero-Thermo-Elasticity of Functionally Graded Panels," *Journal of Thermal Stresses*, Vol. 34, pp. 536-568, 2011.

[9] Dunning, P., Stanford, B., Kim, H., Jutte, C., "Aeroelastic Tailoring of a Plate Wing with Functionally Graded Materials," *Journal of Fluids and Structures*, Vol. 51, pp. 292-312, 2014.

[10] Stanford, B., Jutte, C., Wieseman, C., "Trim and Structural Optimization of Subsonic Transport Wings using Nonconventional Aeroelastic Tailoring," *AIAA Journal*, Vol. 54, No. 1, pp. 293-309, 2016.

[11] Deaton, J., Grandhi, R., "A Survey of Structural and Multidisciplinary Continuum Topology Optimization: Post 2000," *Structural and Multidisciplinary Optimization*, Vol. 49, No.1, pp. 1-38, 2014.

[12] Stanford. B., "Aeroelastic Wingbox Stiffener Topology Optimization," *Journal of Aircraft*, to appear.

[13] Vassberg, J., DeHaan, M., Rivers, S., Wahls, R., "Development of a Common Research Model for Applied CFD Validation Studies," *AIAA Applied Aerodynamics Conference*, Honolulu, Hawaii, August 10-13, 2008.

[14] Stanford, B., Jutte, C., Coker, C., "Sizing and Layout Design of an Aeroelastic Wingbox through Nested Optimization," *AIAA SciTech Forum*, Kissimmee, Florida, January 8-12, 2018.

[15] Dunning, P., Stanford, B., Kim, H., "Coupled Aerostructural Topology Optimization using a Level Set Method for 3D Aircraft Wings," *Structural and Multidisciplinary Optimization*, Vol. 51, No. 5, pp. 1113-1132, 2015.

[16] Gaynor, A., Guest, J., "Topology Optimization Considering Overhang Constraints: Eliminating Sacrificial Support Material in Additive Manufacturing through Design," *Structural and Multidisciplinary Optimization*, Vol. 54, No. 5, pp. 1157-1172, 2016.